Acta Cryst. (1963). **16**, 338

The Crystal Structure and Powder Data for Arsenic Telluride

By Gene J. Carron

Research Division, McDonnell Aircraft Corporation, St. Louis, Missouri, U.S.A.

(*Received* 21 *March* 1962 *and in revised form* 11 *June* 1962)

The crystal structure of the semiconducting compound As_2Te_3 has been determined from diffractometer and Weissenberg data taken on single crystals. The unit cell is monoclinic and the space group is C_{2h}^3–$C2/m$. The atoms occupy five sets of special positions 4(i): $(x, 0, z)(\bar{x}, 0, \bar{z}) +$ $(000, \frac{1}{2}\frac{1}{2}0)$. There are four molecules per unit cell. The parameters are:

$$a = 14{\cdot}339 \pm 0{\cdot}001,\ b = 4{\cdot}006 \pm 0{\cdot}005,\ c = 9{\cdot}873 \pm 0{\cdot}005\ \text{Å};\ \beta = 95{\cdot}0°.$$

The structure, which consists of zigzag chains in which the arsenic atoms are octahedrally and trigonally bonded to telluriums, appears closely related to the structure of β-Ga_2O_3. Complete powder data for arsenic telluride are included.

1. Introduction

Crystallographic data obtained from Weissenberg photographs of very small single-crystal fragments of As_2Te_3 were reported by Singer & Spencer (1955). The crystals, in their investigation, were prepared by reacting stoichiometric quantities of reagent-grade elements in evacuated quartz and then cooling the melt directionally. Their report indicated As_2Te_3 to be monoclinic, with 4 molecules/unit cell. Its space group was reported to be Cm ($0k0$ data lacking) and lattice parameters

$$a = 14{\cdot}4,\ b = 4{\cdot}05,\ c = 9{\cdot}92\ \text{Å};\ \beta = 97°.$$

In the course of investigations on various thermoelectric materials in this laboratory, single crystals of As_2Te_3, approximately 0·5 cm. by 4 cm. were prepared. In order to gain a better understanding of the crystal chemistry of the various ternary compounds derived from As_2Te_3, a determination of the structure of this compound was made. Arsenic telluride contains a predominate cleavage indicative of weak bonds. It was felt that this might be ascribed to weak Te–Te bonds similar to those reported in the Bi_2Te_3 structure by Drabble & Goodman (1958).

2. Experimental

The compound was formed by reacting high purity elements (99·999%) in an evacuated quartz crucible. Homogenization was ensured by placing the crucible and its contents in a rocking furnace. Subsequent single-crystal growth was achieved by the Bridgman technique. Taking the y axis as the unique axis, the crystals showed preferential growth in the [010] direction and exhibited strong cleavage parallel to the (100) face.

Several small single crystalline fragments cleaved from the prepared specimens from different growth runs were examined on the G.E. XRD-5 unit using the single-crystal orienter (Furnas, 1957) and Ni filtered Cu radiation. Data were collected on ($h00$), ($0k0$), ($00l$), ($hk0$), and (hkl) reflections. Peak intensities were obtained on all observed reflections. The structure is monoclinic and systematic absences, hkl, $h+k \neq 2n$, are consistent with the space groups $C2$, Cm, and $C2/m$.

Lattice constants obtained are

$$a = 14{\cdot}339 \pm 0{\cdot}001,\ b = 4{\cdot}006 \pm 0{\cdot}005,$$
$$c = 9{\cdot}873 \pm 0{\cdot}005\ \text{Å};\ \beta = 95{\cdot}0°;$$
$$\text{calc. cell volume} = 564{\cdot}96\ \text{Å}^3;$$
$$d(\text{calc.}) = 6{\cdot}26,\ d(\text{obs.}) = 6{\cdot}25\ \text{g.cm.}^{-3};$$
$$4\ \text{molecules per unit cell}.$$

Numerous small (approximately 1 mm. length) single crystals suitable for morphological examination were obtained from a fractured section of a polycrystalline ingot. This ingot had been quenched rapidly after a failure in the control of the Bridgman furnace. The ingot contained several internal voids each of which contained a cluster of well developed crystals growing around it. Several of these crystals were carefully removed and cemented to glass fibers. The mounted crystals were first examined on the single crystal orienter. A sufficient number of reflections were recorded to permit calculation of lattice constants and to determine the position of the crystallographic axes relative to the external faces visible on the crystals. These diffractometer results were in very good agreement with the X-ray data collected on the crystal fragments thus substantiating the identity between the two crystal specimens. The small crystals were next mounted on a two-circle reflecting goniometer. Angular measurements were recorded on pinacoidal, hemi-orthodomes, and hemi-bipyramidal faces. Polar plots of the reflections indicated the existence of a two-fold symmetry axis. Unfortunately, due to the growth nature of the specimens, no informa-

tion could be obtained by this method on the existence of a symmetry plane.

To supplement the diffractometer data, zero layer (*h*0*l*) Weissenberg photographs were taken of one of the small crystals. Both Cu and Mo radiation were employed using a multiple film technique. The intensities were estimated, and corrected for both absorption and Lorentz-polarization. Absorption correction factors applied were those by Bond (1959) for cylindrical specimens assuming an average radius of 0·05 mm.

3. Structure determination

As previously noted the systematic absences are consistent with the space groups $C2$, Cm, and $C2/m$. The two-fold symmetry axis revealed in the morphological examination eliminates Cm from consideration. In the general positions of $C2/m$, and the special positions e through h of $C2/m$ (Lonsdale & Henry, 1952) the symmetry plane would require that equivalent atoms be spaced at a maximum distance of 2·00 Å. This packing limitation would not appear possible since the Te–Te bond distance in tellurium metal is 2·896 Å.

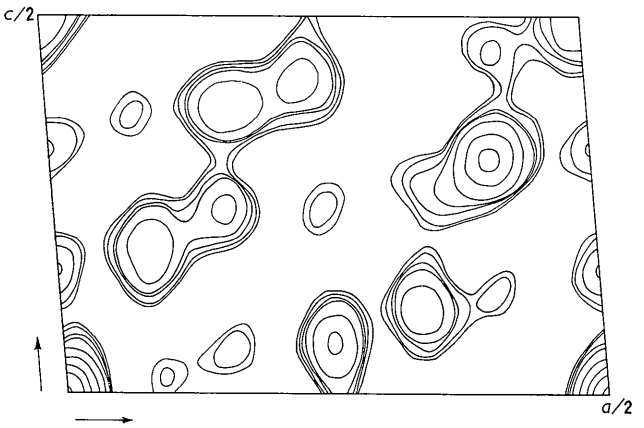

Fig. 1. Patterson projection, $P(x, z)$.

Considering then the possibilities of $C2$ and the special positions $4i$ of $C2/m$ which project on the xz plane as $p2$, two-dimensional Patterson syntheses were made independently using the (*h*0*l*) diffractometer intensities, and the (*h*0*l*) Weissenberg intensities. The two plots were in excellent agreement considering that there were no absorption corrections applied to the diffractometer intensities. The diffractometer Patterson computations were performed on an IBM 650 computer and the Weissenberg Patterson on an IBM 7090. Fig. 1 shows the Patterson projection obtained from the Weissenberg data.

The short b lattice distance minimized the possibility of superpositioning; therefore, the more intense maxima were considered to be due to Te–Te interactions. Based on this supposition and a plot of the more intense (*h*0*l*) reflections, preliminary xz coordinates were assigned to the atoms. Phase calculations were made for the (*h*0*l*) reflections and an electron density Fourier synthesis carried out on the IBM 7090.

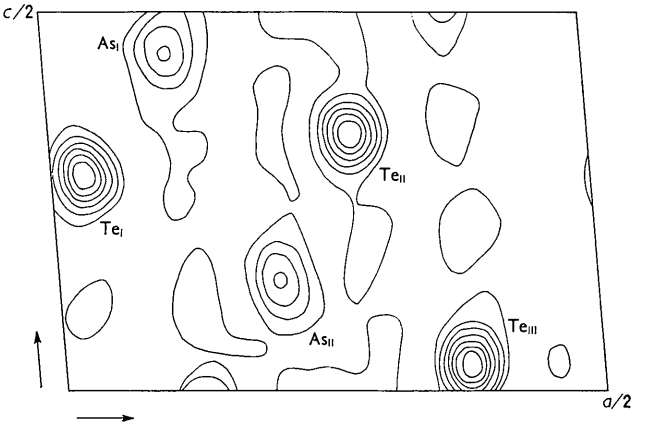

Fig. 2. Electron-density projection, $\varrho(x, z)$. Contours are drawn at equal intervals.

Successive Fourier syntheses were made using improved coordinates. The final electron density projection shown in Fig. 2 clearly differentiated between the tellurium and arsenic positions. The diffractometer data indicated similar intensity distributions on layers 0, 2, 4, 6 ... and 1, 3, 5, 7 ... along the b axis. This fact, plus the consideration of possible positions for reinforcement of the stronger (*hk*0) reflections, led to the conclusion that the structure was layered at 0 and $\frac{1}{2}b$. The arsenic and tellurium atoms, most likely, occupying five special positions $4i$ in $C2/m$, namely, $x, 0, z$; $\bar{x}, 0, \bar{z}$; $+(0, 0, 0; \frac{1}{2}, \frac{1}{2}, 0)$.

Table 1. *Atomic positional parameters*

	x	y	z
As_I	0·115	0·5	0·445
As_{II}	0·205	0·0	0·145
Te_I	0·032	0·0	0·282
Te_{II}	0·280	0·5	0·337
Te_{III}	0·375	0·0	0·034

Table 1 lists the atomic positional parameters from the final Fourier synthesis. No further attempt was made to refine these values. Calculated and observed structure factors are given in Table 2 for (*h*0*l*) and (*hk*0) reflections. A temperature factor, $\exp -B(\sin^2\theta/\lambda^2)$ with $B=2{\cdot}5$, was applied to the (*h*0*l*) calculated structure factors. These corrected (*h*0*l*) factors are compared to the observed values from the Weissenberg data after the latter were corrected for absorption and Lorentz-polarization. To verify the y positional coordinate the (*hk*0) diffractometer data, corrected for absorption and Lorentz-polarization, were used. The temperature factor applied to the calculated $F(hk0)$ factors used a value of $B=4{\cdot}0$. Computing the reliability factor,

Table 2. *Observed and calculated structure factors for* As_2Te_3

hkl	$\lvert F_o\rvert$*	F_c	*hkl*	$\lvert F_o\rvert$*	F_c	*hkl*	$\lvert F_o\rvert$*	F_c
200	26·5	−22·3	10,0,0	17·5	+18·8	$\bar{8}01$	53·5	+48·1
201	18·0	−19·8	10,0,6	42·5	+48·0	$\bar{8}04$	80·0	+77·3
204	102·9	+112·5	10,0,7	22·5	+23·3			
206	16·5	+13·3	10,0,8	10·0	−10·2	$\bar{10}$,0,3	42·0	−33·6
207	43·5	+44·8	10,0,9	25·5	+19·7	$\bar{10}$,0,4	41·5	−49·1
209	10·0	−12·2	12,0,0	68·0	−64·1	$\bar{10}$,0,5	15·5	+18·9
2,0,10	31·5	+34·8	12,0,1	50·0	−36·4	$\bar{10}$,0,6	39·5	−31·5
2,0,11	15·0	+23·0	12,0,2	20·0	+16·9	$\bar{10}$,0,7	14·5	−21·8
2,0,12	6·5	−12·7	12,0,3	20·5	−16·8			
			12,0,4	20·5	−15·6	$\bar{12}$,0,1	23·0	+21·3
401	68·0	−71·5	12,0,5	8·5	+7·1	$\bar{12}$,0,2	30·0	−21·7
402	32·5	−36·0	12,0,7	17·5	−19·2	$\bar{12}$,0,3	23·0	−22·6
403	35·0	+35·9				$\bar{12}$,0,4	10·0	+3·8
404	57·0	−67·8	14,0,4	25·5	−33·0	$\bar{12}$,0,6	32·0	−27·1
405	50·0	−55·2	14,0,5	16·5	−13·2			
406	24·0	+22·9	14,0,7	16·5	−14·6	$\bar{14}$,0,5	36·5	+24·7
407	16·5	−10·0				$\bar{14}$,0,6	32·5	+34·9
408	16·5	+17·3	16,0,0	7·0	−9·0			
409	10·0	+4·8	16,0,1	8·5	+11·7	$\bar{16}$,0,1	32·0	+19·5
4,0,10	12·5	+11·2	16,0,2	22·0	+19·0	$\bar{16}$,0,2	39·0	+38·9
4,0,11	12·0	+4·9	16,0,5	18·0	+25·1	$\bar{16}$,0,3	11·0	−10·3
						$\bar{16}$,0,4	13·0	+10·1
602	63·0	−69·3	$\bar{2}02$	36·5	−24·2			
604	14·0	−16·1	$\bar{2}05$	16·5	−12·9	003	72·5	+62·3
605	26·5	−32·4	$\bar{2}06$	114·0	−102·4	005	25·5	−24·5
607	11·0	+13·2	$\bar{2}08$	11·0	−5·3	006	26·5	+28·8
608	46·5	−49·9	$\bar{2}09$	32·5	−39·0	007	27·0	+34·2
609	22·5	−27·4	$\bar{2}$,0,10	10·0	+3·6	008	16·5	−14·7
6,0,10	8·5	+13·8	$\bar{2}$,0,12	10·0	−17·1	0,0,10	20·0	−26·3
6,0,11	22·0	−18·6				0,0,12	5·0	−9·2
			$\bar{4}02$	160·5	−160·9			
800	51·0	+35·1	$\bar{4}05$	32·0	−30·2	110	5·0	+3·5
801	36·0	−30·9	$\bar{4}06$	16·5	+7·1	310	22·1	+20·9
802	71·5	+81·9	$\bar{4}07$	11·0	+10·2	510	62·2	+62·1
803	42·0	+54·0	$\bar{4}$,0,12	11·0	+24·1	710	32·8	−36·0
804	16·5	−23·4				11,1,0	4·9	−5·8
805	24·5	+34·0	$\bar{6}01$	51·0	+37·9	13,1,0	13·4	+5·2
806	9·5	+2·3	$\bar{6}02$	43·0	+51·8			
807	8·5	−5·8	$\bar{6}03$	16·5	−21·3	220	5·2	−7·0
808	8·5	−8·2	$\bar{6}04$	43·0	+41·2	820	15·4	+11·6
809	7·0	+9·4	$\bar{6}05$	16·5	+24·6	10,2,0	13·5	+6·4
			$\bar{6}08$	57·5	+68·0	12,2,0	21·4	−20·3
			$\bar{6}$,0,11	13·0	+24·7			
			$\bar{6}$,0,12	5·0	−5·6	330	4·9	+8·7
						530	24·8	+27·8
						730	17·1	−16·8
						11,3,0	3·5	−2·9

* Weissenberg intensity data used to determine ($h0l$) $|F_o|$. Diffractometer intensity data used to determine ($hk0$) $|F_o|$.

$$R=\Sigma||F_o|-|F_c||/|F_o|$$

disregarding unobserved reflections, values of $R(h0l)=0{\cdot}177$ and $R(hk0)=0{\cdot}146$ were obtained. Even considering the effect of the unobserved reflections on these values, it is believed that these R values indicate fair agreement between the observed and calculated structure factors. The accuracy of the estimated intensities was affected by the high absorption coefficient of As_2Te_3 for Cu radiation.

4. Description of the structure

A (010) plan view of the proposed As_2Te_3 structure is shown in Fig. 3 and the calculated interatomic distances listed in Table 3. The structure consists

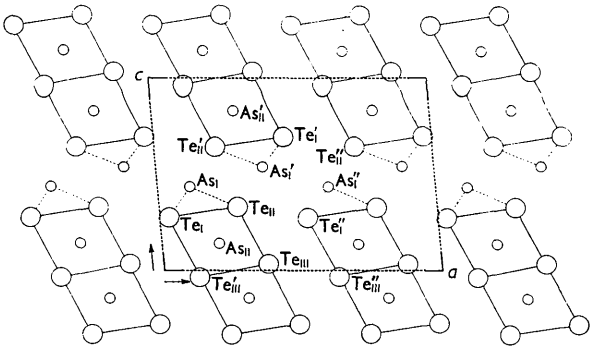

Fig. 3. Plan view of As_2Te_3 proposed structure. Large circles are Te sites, smaller circles are As sites. Unit cell is indicated by heavy dotted line.

Table 3. *Interatomic distances*

	Atom pair (no.)	Distance
$As_{II}Te_6$ octahedron	Te_I–Te_{II} (2)	4·07 Å
	Te_{II}–Te_{III} (2)	3·94
	Te_{II}–Te_{III}' (2)	4·11
	Te_I–Te_{III}' (2)	4·03
	Te_{II}–Te_{II}	4·01
	Te_{III}'–Te_{III}'	4·01
	Te_{II}–Te_{III}' (2)	4·01
	As_{II}–Te_I	2·93
	As_{II}–Te_{III}	2·76
	As_{II}–Te_{II} (2)	2·90
	As_{II}–Te_{III}' (2)	2·85
As_I trigonal pyramid	Te_I–Te_{II} (2)	4·07
	Te_I–Te_{II}' (2)	4·43
	Te_{II}–Te_{II}' (2)	3·95
	Te_I–Te_I	4·01
	Te_{II}'–Te_{II}'	4·01
	As_I'–Te_I'' (2)	4·09
	As_I'–Te_{II}'' (2)	5·23
	As_I'–As_I''	3·56
	As_I–Te_{II}	2·68
	As_I–Te_I (2)	2·77
	As_I–Te_{II}' (2)	3·22
Between chains	Te_{II}–Te_I''	3·70
	Te_{III}–Te_{III}''	3·70
	Te_{III}–Te_I'' (2)	3·75
Shortest As–As distances	As_I–As_{II} (2)	3·89
	As_{II}–As_I'	4·61
	As_I'–As_I''	3·56
	As_I–As_I' (2)	4·41
	As_I–As_I (2)	4·01
	As_{II}–As_{II} (2)	4·01
	As_{II}–As_{II}' (2)	3·81
Averages	Te–Te between chains	3·72
	Te–Te octahedron	4·04
	Te–Te trigonal pyramid	4·05
	$As_{II}Te$ octahedron	2·86
	As_ITe trigonal pyramid	2·74

essentially of two non-equivalent arsenic positions and three non-equivalent tellurium positions. The As_{II} site is octahedrally coordinated by Te atoms: one Te_I at 2·93 Å, two Te_{II} at 2·90 Å, one Te_{III} at 2·76 Å and two Te_{III}' at 2·85 Å. There are two adjacent octahedra aligned in approximately the [103] direction, which share edges (Te_{III}–Te_{III}') and which are off-set from each other by $\frac{1}{2}b$. In the b direction the octahedra are stacked one on another, sharing edges (Te_{III}'–Te_{II}). Comparison between the average As_{II}–Te octahedral distance of 2·86 Å and the As_I–Te distances indicates that the As_I atoms are strongly bonded to only three neighboring tellurium atoms in a trigonal pyramid configuration. These pyramidal bonds are namely, As_I–Te_{II} at 2·68 Å and As_I–Te_I (2) at 2·77 Å, yielding an average of 2·74 Å. The relatively larger distances, As_I–Te_{II}'' (2), As_I–Te_I'' (2), and As_I–Te_{II}' (2), equal to 5·23 Å, 4·09 Å and 3·22 Å, respectively, preclude the existence of strong bonds between these atoms. It appears, therefore, that the only attractive forces between the staggered chains in the [100] direction are of the weak van der Waals type. This weak attraction between chains is certainly not unique with this structure, for A_2B_3 type compounds, and corresponds to the observed cleavage parallel to the (100) face. The average Te–Te distance between the chains, equal to 3·72 Å, is in very close agreement with the Te–Te distance found between chains in the Te metal structure (3·74 Å). In Te metal the forces between chains are also considered to be van der Waals.

It is necessary now to consider the possible attractive forces existing between the As_I trigonal pyramids along the zigzag chains. The nature of the forces, in this case, is less evident, and it is doubtful that a simple explanation can be put forth. Assuming that the trigonal As_I bonds are of the p^3 type, then there still remain two electrons in the $4s^2$ state, attached to each As_I atom. These electrons may result in a weak bonding to the Te_{II}' atoms. Partial bonding is indicated, possibly, by the interatomic distance As_I–Te_{II}' (2) at 3·22 Å which is considerably smaller than the As_I–Te distances, previously mentioned, between chains. More positive confirmation for these partial bonds is in the crystal itself which displays no evident cleavage or weakness parallel to the (001) face. It is not unlikely that the partial bonds involve a slight ionic contribution. A charge force on each pyramid might result in a staggered pattern as displayed in this structure.

In this proposed structure each Te_I atom is bonded to two As_I atoms (2·77 Å distance) and one As_{II} atom (2·93 Å distance). Te_{II} atoms are bonded to two As_{II} atoms (2·90 Å distance) and one As_I atom (2·68 Å distance) and finally, the Te_{III} atoms are bonded to three As_{II} atoms (2·76 Å and 2·85 Å (2) distance).

5. Comparison with related structures and discussion

There is a marked similarity between the structure proposed herein for As_2Te_3 and that proposed by Geller (1960) for β-Ga_2O_3. In the β-Ga_2O_3 structure we find two non-equivalent Ga sites and three non-equivalent oxygens. The one gallium position is practically identical to the As_{II} site, being octahedrally coordinated in two adjacent octahedra. In Ga_2O_3, however, the second Ga atom is tetrahedrally coordinated between the octahedral chains. This is the obvious tie that is lacking in As_2Te_3, leaving a practically open tunnel between the zigzag chains, as evidenced in the micaceous nature of the crystals. Both Ga and As exhibit a +3 valency in these compounds. In the case of Ga this can occur by sp^2 hybridization. Arsenic on the other hand, with 3 valency electrons in the $4p$ state, has two additional electrons in the $4s^2$ state. These two electrons may account for the structural discontinuity of As_2Te_3 as compared to β-Ga_2O_3.

Another compound, the structure of which is as yet unpublished, that is very likely closely related to As_2Te_3 and β-Ga_2O_3, is α-Ga_2S_3. In the unit cell data published for α-Ga_2S_3 by Goodyear *et al.* (1961), the

structure is reported to have monoclinic symmetry, with a unit cell, centered on the C face, containing 4 molecules.

Several structures can be cited in which arsenic and tellurium atoms have coordinations comparable to the As_2Te_3 structure. There are the monoclinic structures of Orpiment (As_2S_3) and Claudetite (As_2O_3). The structure of Orpiment (Morimoto, 1949) is composed of As_2S_3 layers parallel to the (010), in which each arsenic is surrounded by 3 sulfurs, and each sulfur shared by 2 arsenics. Similarly in Claudetite (Frueh, 1951) the coordination of arsenic is to 3 oxygen atoms. Both of these structures belong to the space group $P2_1/n(C_{2h}^5)$. In the case of tellurium, the Bi_2Te_3 structure (Drabble, 1958) has bismuth atoms with nearly octahedral coordination to tellurium.

Electron diffraction has been employed to study the structure of thin amorphous films of As_2Te_3 (Andrievskii *et al.*, 1962). It was found that the structure changed sharply with the inception of crystallization and that therefore there is little analogy between the two structures (amorphous–crystalline).

6. Powder data

Powder specimens were made from crystal fragments identical with the single crystal studies. These were then examined in a 114·6 mm. Straumanis-loading, Debye–Scherrer camera using Ni filtered Cu radiation.

The pattern obtained was indexed very readily with the aid of the single-crystal data. For the calculated d values the lattice constants from the single-crystal investigation were used. The d values and relative intensities are given in Table 4.

Table 4. *Powder diffraction data for* As_2Te_3

hkl	d_o (Å)	d_c (Å)	I	*hkl*	d_o (Å)	d_c (Å)	I	*hkl*	d_o (Å)	d_c (Å)	I
200	7·07	7·14	*w*	$31\bar{4}$	1·967	1·974	*ms*	207	1·353	1·357	*w*
				005		1·969		10,0,3		1·353	
201	5·54	5·55	*w*	$51\bar{3}$		1·964		$40\bar{7}$		1·349	
				021		1·962					
$20\bar{2}$	4·19	4·23	*w*					820	1·333	1·332	*w*
				513	1·829	1·837	*w*	$82\bar{1}$		1·331	
$11\bar{1}$	3·61	3·62	*w*					$11\bar{7}$		1·331	
400		3·57		710	1·811	1·818	*m*				
				$71\bar{1}$		1·813		913	1·303	1·306	*w*
003	3·25	3·28	*s*	$22\bar{2}$		1·810		$31\bar{7}$		1·306	
401		3·27						606		1·299	
				800	1·784	1·785	*w*				
$11\bar{2}$	3·00	3·07	*vs*	$80\bar{1}$		1·784		330	1·281	1·285	*m*
310		3·06						132		1·280	
$40\bar{2}$		3·02		$51\bar{4}$	1·757	1·754	*w*	$33\bar{1}$		1·278	
112		3·00									
$31\bar{1}$		2·97		115	1·738	1·737	*w*	822	1·265	1·266	*m*
								$22\bar{6}$		1·264	
203	2·87	2·89	*w*	023	1·706	1·709	*w*	$80\bar{6}$		1·264	
311		2·88		421		1·707		$82\bar{3}$		1·264	
402	2·76	2·78	*vw*	$42\bar{2}$	1·667	1·668	*m*	11,1,$\bar{1}$	1·238	1·238	*w*
				405		1·664		332		1·236	
312	2·527	2·538	*m*	712		1·664		11,1,0		1·235	
$11\bar{3}$		2·528									
$40\bar{3}$		2·528		514	1·628	1·633	*m*	914	1·222	1·222	*w*
				802		1·633		$42\bar{6}$		1·222	
510	2·316	2·325	*s*	$20\bar{6}$		1·630		11,1,$\bar{2}$		1·222	
403		2·317		$80\bar{3}$		1·629					
$31\bar{3}$		2·305		422		1·624		530	1·208	1·209	*w*
$51\bar{1}$		2·300						823		1·208	
				$80\bar{4}$	1·505	1·509	*m*	10,0,$\bar{5}$		1·207	
204	2·261	2·267	*m*	621		1·501					
601		2·268		224		1·501		$53\bar{2}$	1·185	1·185	*vw*
511	2·213	2·228	*vw*	406	1·442	1·444	*m*	12,0,1	1·167	1·169	*vw*
$60\bar{2}$		2·220		911		1·442		607		1·167	
				622		1·440		517		1·167	
313	2·170	2·179	*w*								
$51\bar{2}$		2·163		$60\bar{6}$	1·408	1·409	*vw*	$62\bar{6}$	1·152	1·152	*vw*
				007		1·406		12,0,$\bar{3}$		1·151	
602	2·066	2·073	*m*	$02\bar{5}$		1·404		027		1·151	
114		2·053		$20\bar{7}$		1·403					
512		2·047						227	1·123	1·124	*vw*
				$71\bar{5}$	1·391	1·391	*vw*	533		1·121	
020	2·003	2·003	*m*	804		1·389		10,2,$\bar{3}$		1·121	

vs = very strong, *s* = strong; *ms* = medium strong, *m* = moderate; *w* = weak, *vw* = very weak.

The author wishes to thank Prof. Lindsay Helmholz of Washington University for his aid in the interpretation of the Patterson projections and helpful suggestions throughout the investigation. He is also indebted to Drs W. L. Kester and D. P. Ames of the McDonnell Aircraft Research Division for many informative discussions on the problem.

References

ANDRIEVSKII, A. I., NABITOVICH, I. D. & VOLOSHCHUK, YA. V. (1962). *Soviet Physics, Crystallography*, **6**, 534.
BOND, W. L. (1959). *Acta Cryst.* **12**, 375.
DRABBLE, J. R. & GOODMAN, C. H. L. (1958). *J. Phys. Chem. Solids*, **5**, 142.
FRUEH, A. J., Jr. (1951). *Amer. Min.* **36**, 832.
FURNAS, T. C., Jr. (1957). Gen. Electric Direction 12130A.
GELLER, S. (1960). *J. Chem. Physics*, **33**, 676.
GOODYEAR, J., DUFFIN, W. J. & STEIGMANN, G. A. (1961). *Acta Cryst.* **14**, 1168.
LONSDALE, KATHLEEN & HENRY, N. F. M. (1952). *International Tables for X-ray Crystallography*. Birmingham: The Kynoch Press.
MORIMOTO, N. (1949). *X-rays (Japanese)*, **5**, 115.
SINGER, J. & SPENCER, C. W. (1955). *J. Metals*, **203**, 144.

Acta Cryst. (1963). **16**, 343

The Crystal and Molecular Structure of Bis-biuret-Zinc Chloride

BY MARIO NARDELLI, GIOVANNA FAVA AND GIULIA GIRALDI

Structural Chemistry Laboratory, Institute of Chemistry, University of Parma, Italy

(*Received* 18 *June* 1962)

Crystals of bis-biuret-zinc chloride, $Zn(C_2H_5N_3O_2)_2Cl_2$, are monoclinic, $P2_1/c$:

$$a = 8{\cdot}02,\ b = 7{\cdot}26,\ c = 11{\cdot}54\ \text{Å};\ \beta = 124{\cdot}7°,\ Z = 2\ .$$

The structure, solved by means of three-dimensional Fourier methods, has been refined with anisotropic differential synthesis. The metal atom lies on a symmetry centre and coordinates octahedrally two chlorine atoms (Zn–Cl = 2·53 Å) and two pairs of oxygen atoms (Zn–O_1 = 2·05, Zn–O_2 = 2·03 Å), these last being at the corners of a slightly distorted square. The oxygen atoms belong to two biuret molecules which are in a *cis* configuration with nearly parallel C–O bonds. Steric hindrance between the oxygen atoms causes a slight departure from planarity in the biuret molecule, but each NH_2–CO–NH group itself preserves its planarity. The packing is determined chiefly by the hydrogen bonds NH · · · Cl = 3·24 Å. The probable distribution of the H's has been deduced indirectly and checked by an $F_o - F_c$ synthesis.

The structure of $Zn(C_2H_5N_3O_2)_2Cl_2$ is similar to that of $Cu(C_2H_5N_3O_2)_2Cl_2$ even though these two compounds are not isostructural. Their structures are quite different from that of $Cd(C_2H_5N_3O_2)_2Cl_2$ in which the biuret molecule is in a *trans* configuration and behaves as a monodentate ligand.

Introduction

Some attention has been recently devoted to the structures of biuret metal complexes, these being the simplest compounds in which bonding interactions occur between metal ions and peptides.

The biuret molecule can have various structural configurations when acting as a ligand with metal atoms. The *trans* configuration

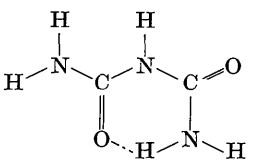

with a strong intermolecular NH · · · O hydrogen bond is present in biuret hydrate (Hughes, Yakel & Freeman, 1961) and it is also likely to occur in dioxane solution, as indicated by the relatively low dipole moment (3·27 D., Kumler, 1959).

The same configuration is preserved practically unchanged in crystals of bis-biuret-cadmium chloride and of bis-biuret-mercury(II) chloride (Cavalca, Nardelli & Fava, 1960); here biuret behaves as a monodentate ligand, and the donor atom is the oxygen atom not involved in hydrogen bonding. The coordination octahedra are linked in endless chains